A NEW MODEL FOR THE MECHANISM OF FISSION OF HEAVY NUCLEI*

By U. Facchini and E. Saetta-Menichella

CISE Laboratories-Segrate (Milano) and Institute of Physical Sciences of the University of Milan**

(Received February 8, 1970; Revised version received May 10, 1970)

A new model of the scission mechanism for fission processes induced by slow and fast neutrons on U^{235} is presented. In this model scission is considered a sudden process; the number of final states in which the fragments can be excited and a suitable scission barrier between the two fragments are taken into account. The experimental data are analyzed and the characteristics of the barrier are discussed.

1. Introduction

Fission of heavy nuclei offers an extensive field for the investigation of nuclear properties. Many aspects of fission such as the existence of the saddle point, the evaporation of neutrons from the excited fragments, the existence of two classes of compound nucleus states, have been investigated and explained, however, a complete description of the whole fission process is still lacking.

In particular the mechanism of the scission of the nucleus into two fragments is not understood. A number of authors (for a review see Wilets [1] and Swiatecki [2]), following the "adiabatic model" predict that the nucleus through a continuous deformation process, assumes the configuration of two fragments connected by a thin neck; the neck becomes thinner and thinner until it breaks and the fragments separate.

The aim of the present work is to offer a different model for scission, based on the hypothesis that the two fragments blow up in a sudden process. In the model the properties of the fragments are predicted by means of a statistical analysis.

In § *2* the basic hypotheses of the model are given. Experimental data are discussed in § *3*; the general statistical formulae are summarized in § *4*. In § *5* the data are analysed and the existence of a potential barrier, acting during the scission, is deduced. Finally the characteristics and the meaning of the barrier are discussed in § *6*.

---

* This work has been performed under the I. N. F. N. — C. I. S. E. collaboration programme.

** Address: C.I.S.E. CASELLA POSTALE 3986, Milano, Italia.

2. *The compound nucleus and the scission process*

2.1. The compound nucleus

As it is well known the fission cross-sections of the nuclei in the Uranium region show a well defined threshold. In 1939 Bohr and Wheeler [3] by means of the liquid drop model, explained this fact as due to the existence of a saddle point in the deformation energy of the nucleus.

In the following years the study of the liquid drop model was thoroughly developed and the total energy of the nucleus was carefully calculated as a function of the deformation parameters [1], [4].

More recently, by the use of corrective terms, which consider the role of single particle states, Strutinsky [5] has shown that the saddle in the total nuclear energy has a structure, *i.e.* there is a well defined minimum after a first maximum, (Fig. 1).

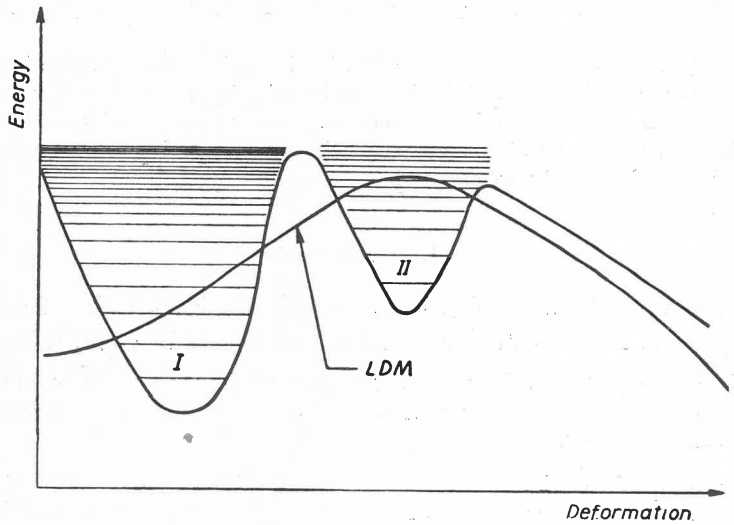

Fig. 1. Two-humped barrier in the deformation energy of a heavy nucleus. In the figure the deformation energy following the liquid drop model (LDM) is also indicated

Experimental evidence of the presence of this second minimum is given by the existence of spontaneously fissioning isomers [6], [7] which are supposed to lie in the very deformed ground state located at the bottom of the second minimum and by the existence of a second class of compound nucleus states corresponding to the very deformed excited nuclei.

An excited U^{236} nucleus, for example, formed in the $U^{235}+n$ reaction, can assume both the compound nucleus states of quasi spherical shape located in the first potential well (I class compound nucleus states) or pass beyond the saddle point and assume the strongly deformed states corresponding to the second minimum (II class compound nucleus states). According to the results of Strutinsky [5] the size of the major axis of the nucleus in the II class states is about $1.5\,R$, R being the radius of the equivalent nuclear sphere.

At around 6 MeV excitation energies the total and fission widths and the densities of the I class compound nucleus states are directly obtained from the analysis of nuclear resonances. The properties of the second class states at excitation energies slightly under the saddle point have been studied recently by Migneco *et al.* [8] and Paya *et al.* [9] by analysing the modulations of the single nuclear resonances.

At higher energies well above the saddle it is possible to hypothesize that the various possible configurations of the compound nucleus are strongly mixed and are in statistical equilibrium with each other.

The average life-time for fission at higher energies can be obtained from the experimental values of the fission cross-section and from the statistical analysis of the properties of the states; these life-times appear to be of the order of 10^{-11}–10^{-15} sec. It appears that the compound nucleus represents a sufficiently stable system which can decay through the scission channels only after a given time even when the total energy of the system is much above the saddle point.

2.2. The fission fragments

From the measurements we know directly the properties of fission fragments, *i.e.* the final states of the system.

In the case of U^{235}+thermal neutrons, the fission energy Q values for the various fragment pairs A_1Z_1, A_2Z_2 are of the order of 180–200 MeV. Most of this energy is found as kinetic energy $\mathscr{E}$ of the fragments, the remaining energy transforms into their excitation energy U. The total average kinetic energy $\overline{\mathscr{E}}$ varies from 155 to 180 MeV for the different fragment pairs and the energy spectra have an almost Gaussian shape with a 15–30 MeV width.

For thermal neutron fission, the total average excitation energy $\overline{U}$ is of the order of 25–35 MeV. It is interesting to note the large number of final channels (formula (4)) corresponding to these excitation energies and that the number of channels varies very sharply with U (from $\sim 10^{12}$ MeV^{-1} for $U = 9$ MeV to $\sim 10^{22}$ MeV^{-1} for $U = 25$ MeV).

2.3. The scission process

We have no direct information on the mechanism of transition from the excited compound nucleus to the system of the two excited fragments. Before discussing the present model we want to cover briefly the description of scission which one gets in the "adiabatic model" and in the "viscous model".

a) The adiabatic model

As reported above, it has been suggested that the nucleus, when beyond the saddle point, turns into the configurations of two fragments connected together by a thin neck; these configurations correspond to the minimum energy of the system, which rapidly decreases as the distance between the centres of the fragments increases (Fig. 2).

The nucleus goes up along these configurations adiabatically until the two fragments split at the scission point: the coulombian repulsion energy of the fragments directly turns into their kinetic energy.

The whole process takes place without phenomena of internal friction and the remaining energy is left as deformation energy of the fragments.

In a successive time when the fragments are completly separate, the deformation energy of the fragments turns into their excitation energy by means of internal friction processes which take place separately in each fragment.

b) The viscous model

Other authors, including Fong [10], state that the adiabatic deformation process takes place very slowly and viscously, so that during deformation, a fraction of the total energy turns directly into internal excitation energy.

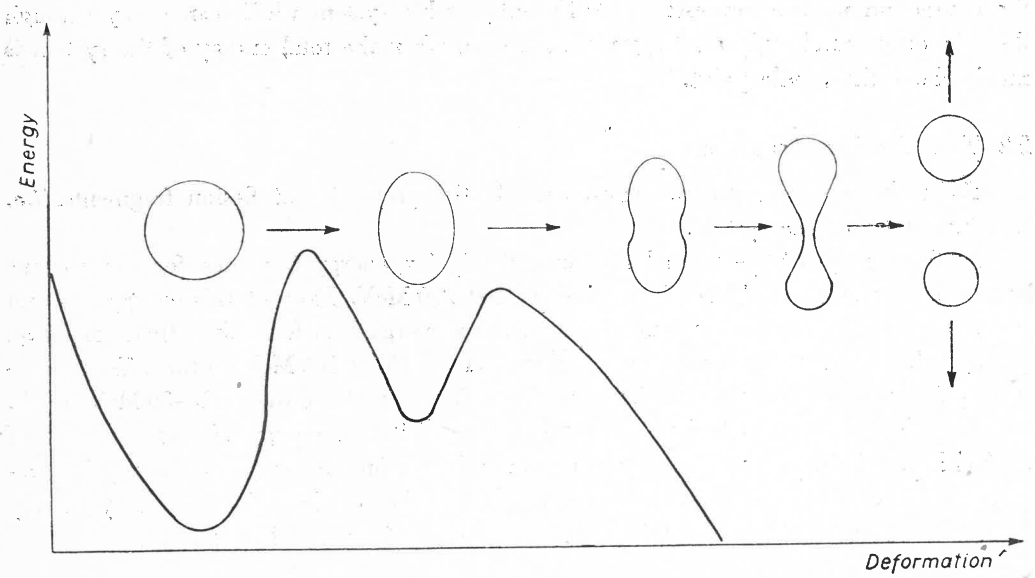

Fig. 2. Representation of the nuclear deformation in the scission process following the adiabatic model

In the "viscous model" the probabilities of the different fission channels are assumed to be proportional to the number of the final states of the excited fragments.

With this model, Fong and recently Ignatiuk [11] have calculated the mass distributions of the fragments in fission of U^{235}+thermal neutrons.

2.4. The sudden model for scission

For this model we must make some basical assumptions:

a) the statistical hypothesis: the compound nucleus life is sufficiently long, for the compound nucleus to face the different final channels with equal probability;

b) the sudden hypothesis: scission takes place through a process in which the two fragments are formed and suddenly blow up from the compound nucleus: the process

is not slow and adiabatic, but rapid and occurs through the peculiar physical conditions which correspond to the formation of two fragments strongly coupled.

The fact that the intermediate configurations do not correspond to the minimum energy curves is very important for the description of the process and will be discussed later;

c) the reversibility hypothesis: the process is reversible, that is the basic configurations assumed in the scission are the same as the ones assumed in the inverse process of fusion of two excited fragments into a given compound nucleus.

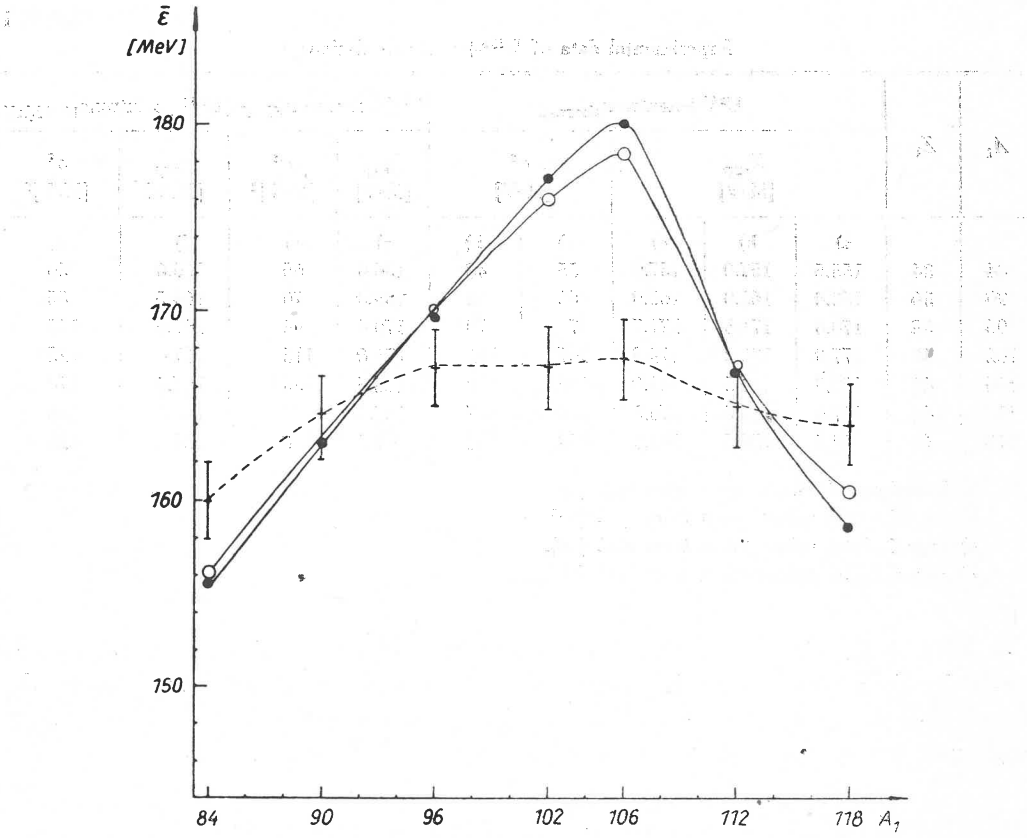

Fig. 3. Values of average total kinetic energies $\bar{\mathscr{E}}$ plotted as function of light fragment mass for fission of U^{235} induced: by thermal neutrons: black points from Ref. [17]; by 6 MeV neutrons: light points from Ref. [17], by 15.5 MeV neutrons: dashed curve with crosses from Ref. [18]

The statistical hypothesis together with reversibility allow the application of the "detailed balance" formula to the entire scission process.

These formulae were studied by Ericson [12] in 1960 and they predict that the values of fission widths are proportional to the number of the final channels multiplied by $T(\mathscr{E})$ the probability of the inverse process of fusion of two excited fragments A_1Z_1, A_2Z_2 with kinetic energy $\mathscr{E}$ into the compound nucleus.

Knowledge of $T(\mathscr{E})$ requires detailed knowledge of the whole process of collision and fusion, but these processes are complicated and have not been sufficiently analysed either in experiment or theory.

In the present paper we obtain the analitical expresion of $T(\mathscr{E})$ from a thorough analysis and fitting of the experimental data. This method was proposed earlier, in 1963, by Facchini *et al.* [13], who obtained empirical expressions for $T(\mathscr{E})$, which have been successively interpreted as transparencies of a suitable potential barrier [14].

TABLE I

Experimental data of U^{235}+ neutrons fissions

A_1	Z_1	U^{235}+neutrons$_{thermal}$					U^{235}+neutrons$_{6MeV}$		U^{235}+neutrons$_{15.5\,MeV}$	
		$\bar{\mathscr{E}}_{exp}$ [MeV]			σ^2 [MeV]		$\bar{\mathscr{E}}_{exp}$ [MeV]	σ^2 [MeV]^2	$\bar{\mathscr{E}}_{exp}$ [MeV]	σ^2 [MeV]^2
		a)	b)	c)	a)	b)	a)	a)	d)	d)
84	34	155.5	157.0	157.9	55	48	156.0	65	160.0	50
90	36	163.0	165.0	165.0	65	58	163.0	70	164.5	85
96	38	170.0	171.5	171.7	75	70	170.0	85	167.0	135
102	40	177.0	180.0	179.8	107	102	176.0	115	167.0	125
106	42	180.0	180.5	181.0	120	110	178.5	135	167.5	170
112	44	167.0	165.5	170.3	180	187	167.0	140	165.0	140
118	46	158.5	156.5	161.0	160	144	160.5	110	164.0	120

a) Experimental values taken from Ref. [17],
b) Experimental values taken from Ref. [15],
c) Experimental values taken from Ref. [16],
d) Experimental values taken from Ref. [18].

We wish to point out, that the present model is completely different from the viscous model by Fong even though, in both cases, the number of the final channels enters the calculations as an important term. It is sufficient to note that the viscous model by Fong undergoes a very slow process, not a sudden one as in the present case.

3. *Experimental data*

Analysis is made of U^{235} fission induced by thermal neutrons and by neutrons of 6 and 15.5 MeV respectively. Correspondently the U^{236} compound nucleus results excited for 6.5, 12.5 and 22 MeV.

The experimental data considered are the following: the kinetic energy spectra, the average excitation energy, the mass spectra, the absolute values of fission widths.

3.1. The kinetic energy spectra

The kinetic energy spectra have been measured by various authors and are well in agreement with each other [15], [16], [17].

We have collected results of Vorobeva *et al.* [17] for fission of U^{235} induced by thermal and 6 MeV neutrons and of Dyachenko and Kuzminov [18] for 15.5 MeV neutrons.

The data for incident neutrons of 6 MeV and of 15.5 MeV must be corrected for the effects of the secondary fission (n, nf) and $(n, 2nf)$. The correction has been made [18] and produces a remarkable change in the results for the data at 15.5 MeV.

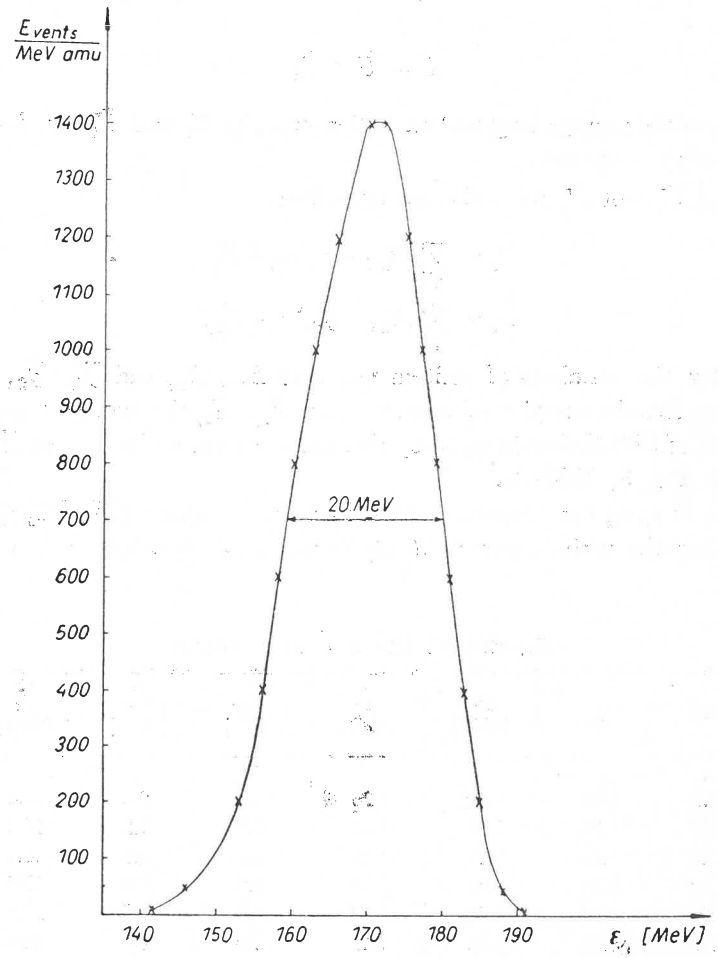

Fig. 4. Total kinetic energy spectrum for thermal fission of U^{235}; fragment pair $A_1 = 96$; $A_2 = 146$, Ref. [15]

For convenience, the values of total average kinetic energies $\overline{\mathscr{E}}$ by reference [17], [18] are given in Fig. 3. Table I collects the total average kinetic energies $\overline{\mathscr{E}}$ of the various authors and at the various energies [15], [16], [17], [18] and the values of σ^2, variance of the total kinetic energy distributions obtained by these authors.

A total kinetic energy spectrum [15] is represented in Fig. 4.

3.2. The Q fission energy and the excitation energy

The Q values for fission of U^{236} in the different fragment pairs have been calculated by various authors; we refer to the tables by Wing and Varley [19]. These values show a relative uncertainty of a few percent.

The Q values can also be obtained from the energy balance of the fission reaction:

$$Q = \overline{\mathcal{E}} + \overline{U}$$

with:

$$\overline{U} = \overline{U}_1 + \overline{U}_2 \tag{1}$$

The values of the average fragment excitation energies $\overline{U}_1$ and $\overline{U}_2$ can be obtained by studying the decay properties.

We get for $\overline{U}_1$ and $\overline{U}_2$ the following formulae:

$$\overline{U}_1 = \sum_i (B_{1ni} + \overline{\mathcal{E}}_{1n}) \nu_{1i} + \overline{E}_{1\gamma}$$

$$\overline{U}_2 = \sum_i (B_{2ni} + \overline{\mathcal{E}}_{2n}) \nu_{2i} + \overline{E}_{2\gamma}$$

ν_{1i}, ν_{2i} being the numbers of emitted neutrons B_{1n}, B_{2n} and $\overline{\mathcal{E}}_{1n}$, $\overline{\mathcal{E}}_{2n}$ the binding and the average kinetic energies of neutrons and $\overline{E}_{1\gamma}$, $\overline{E}_{2\gamma}$ the average γ ray energy.

In the case of U^{236} fission induced by thermal neutrons, we have used $\overline{\mathcal{E}}$ values from Refs [17], [18] (Fig. 3; Table I).

The values of ν_1, ν_2 have been measured by various authors [20], [21], [22], [23] the agreement among the various measurements is not good especially in the zones of the

TABLE II

Experimental data of n and γ emission

A_1	$\bar{\nu}_1$	$\bar{\nu}_2$	$\bar{\mathcal{E}}_{1n}$ [MeV]	$\bar{\mathcal{E}}_{2n}$ [MeV]	$\overline{E}_{1\gamma}$ [MeV]	$\overline{E}_{2\gamma}$ [MeV]	$\overline{U}_1$ [MeV]	$\overline{U}_2$ [MeV]
84	0.72	2.36	1.30	1.20	3.3	2.6	10.4	18.6
90	1.17	1.71	1.30	1.10	5.0	1.2	14.4	12.6
96	1.48	1.27	1.28	1.20	5.1	1.3	16.4	9.7
102	1.54	0.70	1.30	1.50	5.2	0.8	17.0	6.8
106	1.94	0.37	1.38	1.48	6.3	0.3	21.3	3.6
112	2.60	0.93	1.50	1.49	3.6	3.7	24.6	11.8
118	1.72	1.72	1.33	1.33	3.7	3.7	16.6	16.9

symmetric fission where the intensity of emission is low. It is therefore necessary to take values of ν_1, ν_2 averaged over various experimental results.

These values $\bar{\nu}_1$ and $\bar{\nu}_2$ are collected in Table II.

The B_n values are obtained from the tables of Wing and Fong [19]. The average kinetic energies of neutrons have been measured by Milton and Fraser [23] as well as the γ ray energies E_γ and they are collected in Table II.

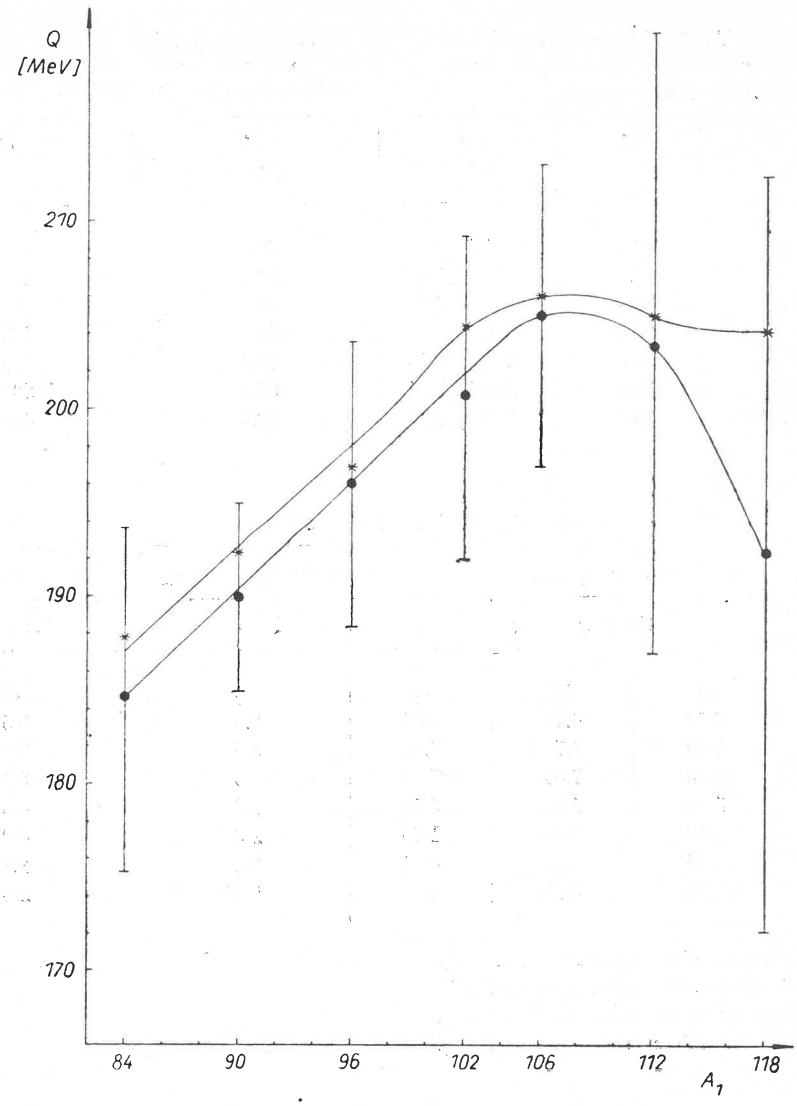

Fig. 5. Comparison of Q values predicted by Wing and Varley [19] indicated by asterisk * with the ones from energy balance indicated by black points

The average $\overline{U}$ values obtained from these calculations are given in Table II.

The Q values are then deduced from the energy balance formula (1) and compared in Fig. 5 with the results by Wing and Fong, the agreement is satisfactory. It is important to note that the Q values, when plotted *versus* A_1 increase up to the pairs in which A_2 is a magic nucleus, then they decrease in the region of the symmetric fission.

The $\overline{U}$ values for fission induced by neutrons with kinetic energy $\mathscr{E}_i$ can be obtained from formula. $\overline{\mathscr{E}}+\overline{U}=Q+\mathscr{E}_i$. They are collected in Table II.

TABLE III

Total pairing energy and total average excitation energy values

	U^{235}+neutrons$_{thermal}$			U^{235}+neutrons$_{6\ MeV}$	U^{235}+neutrons$_{15.5\ MeV}$
A_1	Δ [MeV]	$\overline{U}$ [MeV]	Q [MeV]	$\overline{U}$ [MeV]	$\overline{U}$ [MeV]
84	2.13	29.0	184.5±9.0	34.4	40.0
90	2.48	27.0	190.0±5.0	33.0	41.0
96	2.11	26.0	196.0±7.5	32.0	44.6
102	2.22	23.8	200.8±8.5	30.7	49.2
106	2.15	24.9	204.9±8.5	30.4	51.0
112	2.50	36.4	203.4±16.5	34.4	53.9
118	2.78	33.8	192.3±21.0	38.0	43.8

TABLE IV

Mass distribution experimental data

	U^{235}+neutrons$_{therm\ a}$			U^{235}+neutrons$_{6\ MeV}$	U^{235}+neutrons$_{15.5\ MeV}$
A_1	Pm (%)			Pm (%)	Pm (%)
	a)	b)	c)	a)	d)
84	0.50	0.85	0.45	0.5	0.5
90	3.50	3.70	3.40	3.5	2.4
96	6.80	7.00	6.60	6.0	3.4
102	5.90	5.50	5.50	5.7	4.0
106	2.40	1.80	1.70	2.8	4.2
112	0.09	0.02	0.04	0.2	2.1
118	0.04	0.014	0.01	0.15	2.0

a) Experimental values taken from Ref. [17].
b) Experimental values taken from Ref. [15].
c) Experimental values taken from Ref. [16].
d) Experimental values taken from Ref. [18].

3.3. The mass spectra

The mass spectra of fission of U^{235}+neutrons have the well known shape with a maximum for the heavy fragment having double closed shells; then the spectra fall rapidly at the wings in both the strongly asymmetric and symmetric regions. This fall reduces when the energy of the incident neutrons increases. It must also be pointed out that in the case of fission induced by fast neutrons the effect of the secondary fission must be taken into account.

The mass spectra adjusted according to the analysis of Dyachenko and Kuzminov [18] are presented in Fig. 6 and the relative values of fission probabilities of the various fragment pairs P_m are collected in Table IV.

3.4 Values of $\frac{\Gamma}{D}$

In the case of fission induced by slow neutrons the values of Γ_f fission widths and the values of D, spacing of the compound nucleus levels, are obtained directly from the measurements of the nuclear reasonances. At higher energies the values can be obtained from formula:

$$\frac{\sigma_f}{\sigma_n} = \frac{\Gamma_f}{\Gamma_n} \frac{\Gamma_{f_0}}{\Gamma_{n_0}} \tag{2}$$

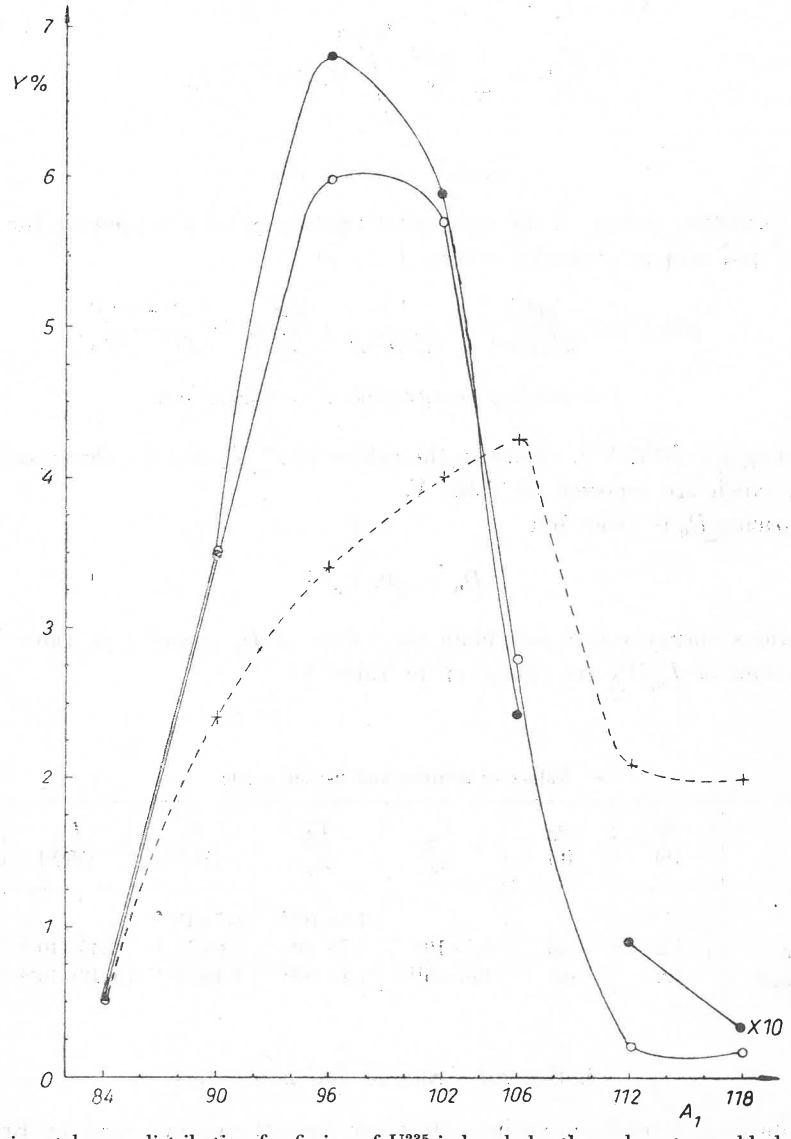

Fig. 6. Experimental mass distribution for fission of U^{235} induced: by thermal neutrons: black points from Ref. [17]; by 6 MeV neutrons: light points from Ref. (17]; by 15.5 MeV neutrons: doshed curve with crosses from Ref. [18]

where σ_f and σ_n are respectively the cross-sections of primary fission and of neutron evaporation and Γ_f and Γ_n represent respectively the fission widths and the neutron widths for a given compound nucleus with a spin I. The Γ_{f_0} and Γ_{n_0} are the corresponding widths for a compound nucleus with spin zero.

The values of σ_f and σ_n at the various incident energies are taken from references [24] [18] and are collected in Table V.

Γ_{n_0} values can be calculated by means of the statistical formula:

$$\frac{\Gamma_{n_0}}{D_0} = \frac{1}{\pi}\frac{mR^2}{\hbar^2}\int_0^{\mathscr{E}_{n\max}} \mathscr{E}_n \varrho(0, U)\, d\mathscr{E}_n \tag{3}$$

$$\mathscr{E}_{n\max} = U_c - \Delta - B_n$$

U_c is the excitation energy of the compound nucleus $\varrho(0, U)$ represents the density of levels with spin zero at excitation energy U

$$\varrho(0, U) = \frac{\varrho(U)}{2^{3/2}\pi^{1/2}\sigma^3} = \frac{1}{2^{3/2}\pi^{1/2}\sigma^3}\cdot\frac{\sqrt{\pi}}{12}\, a^{-1/4}\cdot\frac{e^{2\sqrt{a(U-\Delta)}}}{(U-\Delta)^{5/4}}, \tag{4}$$

Δ = pairing energy and $\sigma^2 = 0.24\, A^{2/3} gt$.

Assuming $a = 30\,\mathrm{MeV}^{-1}$, we obtain the values for Γ_{n_0}/D_0 and the corresponding values for Γ_{f_0}/D_0 which are reported in Table V.

The spacing D_0 is given by:

$$D_0 = \varrho(0, U_c)^{-1}$$

At various energy values we obtain the values of D_0 reported in Table V.

The values of $\Gamma_{n_0}/\Gamma_{f_0}$ are also given in Table V.

TABLE V

Values of neutron and fission widths

	σ_f (b)	σ_n (b)	$\frac{\Gamma_{n_0}}{D_0}$	$\frac{\Gamma_{f_0}}{D_0}$	D_0 [MeV]	Γ_{n_0} [MeV]	Γ_{f_0} [MeV]
$U^{235}+n_{\mathrm{ther}}$	/	/	/	1.5×10^{-2}	6.7×10^{-6}	/	$\sim10^{-7}$
$U^{235}+n_{6\,\mathrm{MeV}}$	1.2	1.8	5.5×10^{4}	3.7×10^{4}	2.6×10^{-10}	1.45×10^{-5}	9.6×10^{-6}
$U^{235}+n_{15.5\,\mathrm{MeV}}$	1.0	0.3	4.4×10^{11}	1.4×10^{12}	1.4×10^{-15}	6.12×10^{-4}	1.97×10^{-3}

4. General formulae and parameters

4.1. The basic formulae used here are taken from the general work by Ericson [12]. The average value of the fission width of a nucleus A having excitation energy U, and spin I, relatively to the scission into two fragments A_1 and A_2 with nuclear charge respectively Z_1

and Z_2 and for a given direction of emission $\vec{n}$, making a δ angle in respect to the direction of the incident neutrons, is given by:

$$\Gamma_{A_1,Z_1;A_2,Z_2}(I, U_c, \vec{n}) = \frac{1}{(2\pi)^{1/2}} \frac{1}{\varrho_c(I, U_c)} \int_0^{Q} T(\mathscr{E}) \int_0^{Q-\mathscr{E}} \varrho_1(U_1)\varrho_2(U_2) \cdot \frac{1}{(\sigma_1^2+\sigma_2^2)^{1/2}} \times$$

$$\times \exp\left(-\frac{I^2 \sin^2\delta}{4(\sigma_1^2+\sigma_2^2)}\right) J_0\left(iI^2 \frac{\sin^2\delta}{4(\sigma_1^2+\sigma_2^2)}\right) dU_1 d\mathscr{E} \tag{5}$$

In this formula $T(\mathscr{E})$ represents the transparency factor between the two fragments for a given total kinetic energy $\mathscr{E}$; ϱ_1 and ϱ_2 are the nuclear state densities of the final fragments at excitation energies respectively U_1 and U_2. $\varrho_c(I, U_c)$ represents the level density of the compound nucleus having spin I and excitation energy U_c.

In the case of low values of spin of the compound nucleus states, we may use a simpler formula, overlooking the slight dependence of the Γ on the δ angle, the total fission width integrated over all the angles and all the possible pairs is then given by:

$$\Gamma_f(I, U_c) = \sum_{A_1Z_1, A_2Z_2} \frac{2}{(2\pi)^{1/2}\varrho_c(I, U_c)} \times$$

$$\times \int_0^{Q} T(\mathscr{E}) \int_0^{Q-\mathscr{E}} \varrho_1(U_1)\varrho_2(U_2) \frac{1}{(\sigma_1^2+\sigma_2^2)^{1/2}} dU_1 d\mathscr{E} \tag{6}$$

with $\varrho_c(I, U_c) = (2I+1)\, e^{-I(I+1)/2\sigma^2}\varrho_c(O, U_c)$.

From this formula the total kinetic energy spectrum of the fission fragment pairs A_1,Z_1 A_2Z_2 is obtained as:

$$P(\mathscr{E}) \alpha T(\mathscr{E}) I(U) = T(\mathscr{E}) \int_0^{Q-\bar{\mathscr{E}}} \varrho_1(U_1)\varrho_2(Q-\mathscr{E}-U_1) dU_1 \tag{7}$$

It is interesting to note that the integral $I(U)$ is maximum for any given value of $U = Q-\bar{\mathscr{E}}$ when the $\frac{d \log \varrho_1}{dU_1} = \frac{d \log \varrho_2}{dU_2}$ *i. e.* when the fragments have the same temperatures.

The total probability to have a given pair A_1Z_1, A_2Z_2 is:

$$\Gamma_{A_1Z_1;\,A_2Z_2}(I, U_c) = \frac{2}{(2\pi)^{1/2}\varrho^c(I, U_c)} \cdot \int_0^{Q-\Delta} T(\mathscr{E}) \int_0^{Q-\mathscr{E}-\Delta} \varrho_1(U_1)\varrho_2(U_2) \frac{1}{(\sigma_1^2+\sigma_2^2)^{1/2}} dU_1\, d\mathscr{E}. \tag{8}$$

We assume in the following that the level densities $\varrho_1(U_1)$ and $\varrho_2(U_2)$ are given with particular values of a_1 and a_2 as in formula (4). It must be noted that a group of heavy fission fragments have double closed shells and the level density of these nuclei slightly deviate from formula (4) due to the effect of the energy gap which is present at the fermi top of the closed shell nuclei. For simplicity we will consider in the following that the law (4) is sufficiently approximate for our calculations.

4.2. Simplification of the integral of levels

The integral of Eq. (7) can be easily simplified by developing the "to be integrated" formula in succession up to the II derivate and assuming for it a gaussian shape.

We have:

$$I(U) = \frac{\pi}{(12)^2}(a_1 a_2)^{-1/4} \int_0^{Q-\bar{\delta}} \frac{e^{2\sqrt{a_1 U_1'}+2\sqrt{a_2 U_2'}}}{U_1'^{5/4}}\, dU_1$$

$$U_1' = U_1 - \Delta_1$$

$$U_2' = U_2 - \Delta_2$$

$$I(U) = \frac{2\pi^{3/2}}{12^2}\frac{a^{5/4}}{a_1 a_2}\frac{e^{2\sqrt{a(Q-\bar{\delta}-\Delta_T)}}}{(Q-\bar{\delta}-\Delta_T)^{7/4}} \quad \text{with } a = a_1 + a_2;\ \Delta_T = \Delta_1 - \Delta_2$$

and then:

$$P(\mathcal{E}) \propto T(\mathcal{E}) I(U)\, \alpha T(\mathcal{E}) \frac{e^{2\sqrt{a(Q-\bar{\delta}-\Delta)_T}}}{(Q-\bar{\delta}-\Delta_T)^{7/4}} \tag{9}$$

This type of simplification has been introduced by Fong and developed by Ignatiuk [11] *et al.*

4.3. Values of a_1, a_2

The authors Erba, Facchini, Saetta-Menichella in 1961 [25] and recently Facchini and Saetta-Menichella in 1968 [26] collected a values for $\approx$200 nuclei and observed that these a values show marked regularities when they are plotted *versus* the mass number A. The a values of the selected nuclei are reported in Fig. 7 in order to show their average behaviour *versus* A. The a values for the fission fragments are not known, because the fragments have a smaller number of protons than the corresponding stable nuclei. Moreover a group of them, namely the fragments of mass around 132 fall in a region where both neutron and proton numbers are magic: $N = 82$, $Z = 50$.

We shall see that the values of a_1 and a_2 referring respectively to the light fragment A_1 and the corresponding heavy fragment A_2 are related (see formula (10')).

As said in § 4.1 the statistical distribution of the excitation energy between the two fragments gives equal temperatures for them. At the maximum value U_i^* of the energy spectra we have:

$$\frac{1}{\vartheta_1^*} = \left(\frac{d \log \varrho_1(U_1)}{dU_1}\right)_{U_1=U_1^*} = \frac{1}{\vartheta_2^*} = \left(\frac{d \log \varrho_2(U_2)}{dU_2}\right)_{U_2=U_2^*} \tag{10}$$

ϑ_1^* and ϑ_2^* being the corresponding temperatures of the two fragments.

The average values $\overline{U}_1$ and $\overline{U}_2$ correspond to U_1^* and U_2^* approximately. From formulae (4) and (10) it follows:

$$\sqrt{\frac{a_1}{\overline{U}_1'}} - \frac{5}{4\overline{U}_1'} = \sqrt{\frac{a_2}{\overline{U}_2'}} - \frac{5}{4\overline{U}_2'}. \tag{10'}$$

When the a_1 value for one fragment is given, from formula (10′) it is possible to obtain the a_2 value of the other fragment. We note from Fig. 7 that the light fragments A_1 are in the region where the a value increases monotonically with the mass number A, but the heavy fragments A_2 are however in a region where there are the double magic closed shells and we must expect particularly low values of a.

Due to these facts we have chosen the a_1 values from interpolation on the curve of Fig. 7 and calculated the a_2 values from formula (10′).

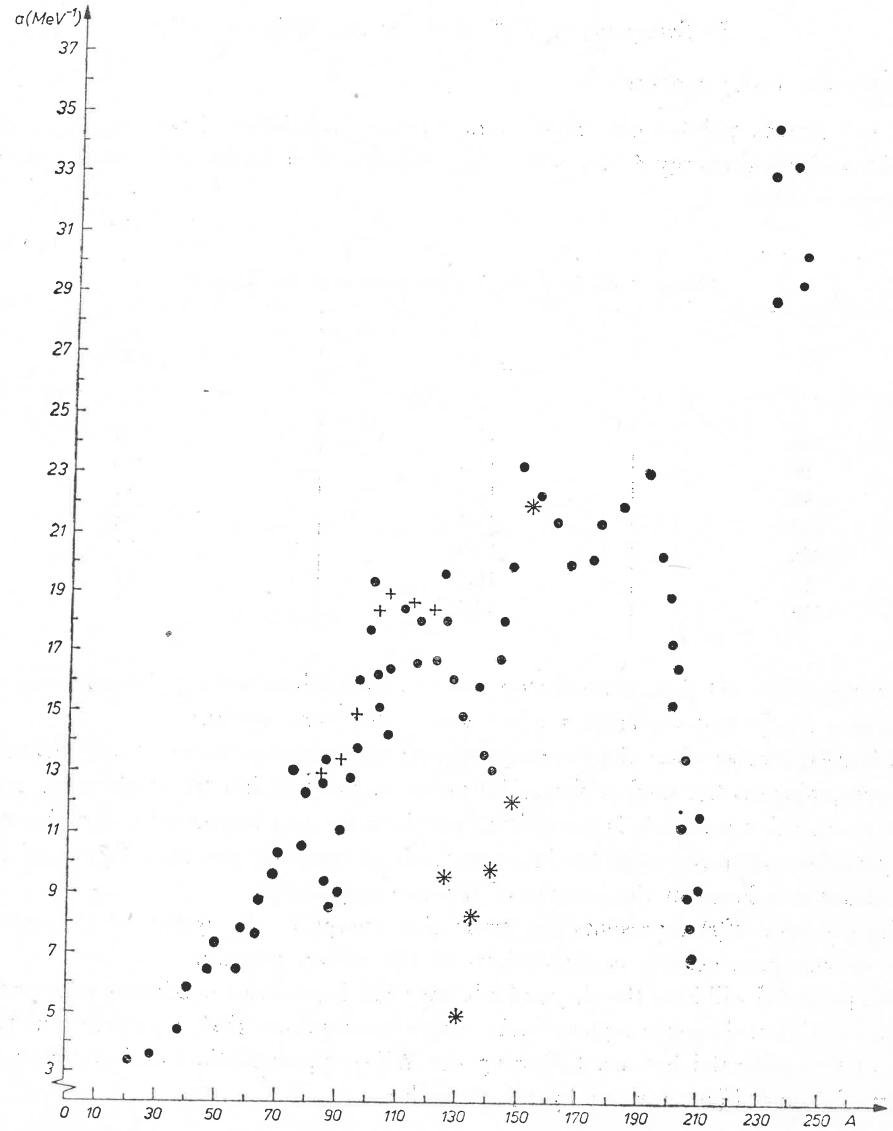

Fig. 7. Values of the level density parameter a distinguished as: black points: selected a values from Ref. [26] and corresponding to stable or neighbouring nuclei, crosses: a_1 values for fission fragments A_1 asterisks: a_2 values for fission fragments A_2, values from the formula (10′)

The a_1 and a_2 values are collected in Table VI and plotted in Fig. 7. It is very important to note that the a_2 values plotted *versus* A give a strong minimum in the region of $N = 82$, $Z = 50$, where the double closed shell nuclei are present. It is very interesting to note that this minimum is quite similar to the minimum already known in the double magic region $N = 26$, $Z = 82$, as can be seen in Fig. 7.

The given values of a are in good agreement with the onescalculated by Lang [27].

5. *Transparency $T(\mathscr{E})$ and the two body potential*

5.1. The two body potential

As was already pointed out, $T(\mathscr{E})$ represents the probability of two fragments A_1, A_2 with relative kinetic energy $\mathscr{E}$ and with total excitation U to collide and coalesce into the compound nucleus.

TABLE VI

Values of the level density parameter a of the fiagments

A_1	a_1 [MeV^{-1}]	a_2 [MeV^{-1}]
84	13.0	21.9
90	13.5	12.3
96	15.0	9.9
102	18.5	8.5
106	19.0	5.1
112	18.7	9.7
118	18.5	18.5

Various forces act during the fusion process: coulombian and repulsive forces, attractive nuclear forces and repulsive nuclear forces (see next section).

At large distances where the two fragments are not in contact there act only the coulombian forces, whereas the nuclear forces intervene in the collision and coalescence regions.

In a simplified model it is possible to consider the two fragments as two interacting single particles and to represent the interaction with a two body potential $V(r)$ as a function of the distance r between the centres of the two fragments.

The potential $V(r)$ represents the interaction energy of the system A_1+A_2 nucleons in the various intermediate configurations of the fusion process.

This potential will have the shape of a barrier which reaches a maximum value and then decreases in the coalescence region; under these assumptions $T(\mathscr{E})$ represents the transparency of this potential barrier. Following the WKB approximation we have the relation between $T(\varepsilon)$ and $V(r)$ as given by the formula:

$$T(\mathscr{E}) = e^{-\frac{2}{\hbar}\int_R^{r_{\mathscr{E}}} \sqrt{2M(V-\mathscr{E})}\,dr} \tag{11}$$

M is the reduced mass of the two separated fragments. The range of integration extends over the barrier thickness.

A few points must be discussed:

a) The potential V and particularly its maximum height B will depend on the fragment pair A_1Z_1, A_2Z_2, for example the coulombian term depends on their charges Z_1Z_2 and the nuclear term may depend on the masses A_1, A_2 and may contain shell effects.

b) The potential describes the transition between the two excited fragments and the compound nucleus and can consequently depend on the particular states in which the compound nucleus is excited, *i. e.* on its excitation energy U_c.

c) The potential $V(r)$ might also depend on the total excitation energy U of the fragments.

This effect cannot be investigated through the proposed procedure. In fact, since the energy U is related to the kinetic energy $\mathcal{E}$ through formula (1), a possible dependence of the $V(r)$ on the excitation energy U will appear in the transparency as mixed and indistinguible from the general $\mathcal{E}$ dependence.

We suppose in the following that, at least in the first approximation the dependence of $V(r)$ on the excitation energy of the fragments is small and does not play an important role.

This conclusion is supported by the results. In fact the shape obtained for $V(r)$ is typical of a fusion process, when the latest views on the coalescence of two big nuclei are considered.

5.2. The expression for $T(\mathcal{E})$

It is possible to obtain the empirical expression for $T(\mathcal{E})$ comparing the experimental energy spectrum of the fission fragments with the statistical formula (7). In this formula the integral describing the level density can be calculated accurately with the given parameters and from comparison between formula and the experimental spectra, the dependence of transparency $T(\mathcal{E})$ *versus* the kinetic energy is obtained. First of all, we can observe that the energy spectrum $P(\mathcal{E})$, represented by formula (7), reaches its maximum value $P(\mathcal{E}^*)$ (correspondingly $U' = U^{*\prime}$)
when

$$\left(\frac{d \log T(\mathcal{E})}{d\mathcal{E}}\right)_{\mathcal{E}=\mathcal{E}^*} = \sqrt{\frac{a}{U^{*\prime}}} - \frac{7}{4U^{*\prime}}. \tag{12}$$

To a good approximation the maximum value of the excitation energy will correspond to its average value $\bar{U}'$ and we have, putting $\left(\frac{d \log T(\mathcal{E})}{d\mathcal{E}}\right)_{\mathcal{E}=\mathcal{E}^*} = \varphi^*$.

$$\varphi^* = \sqrt{\frac{a}{\bar{U}'}} - \frac{7}{4\bar{U}'}. \tag{12}$$

The values of φ^* for the different fragment pairs are collected in Table VII for thermal neutron fission and for fission induced by 6 and 15.5 MeV neutrons repectively. The values of φ^* show a small dependence on the various pairs. The different values of φ^* for the various fragment pairs could represent different shapes of the interaction barrier acting

between the fragments but at the moment the differences in φ^* values cannot be assumed as really meaningful: in fact errors in the measurements and uncertainties in the level density expressions slightly affect these values.

It is interesting to point out that φ^* values reduce with the increase of the total energy of the compound nucleus. The value of the second derivate of log $T(\mathscr{E})$ for $\mathscr{E} = \mathscr{E}^*$ can be obtained by developing into a series, up to the second derivative, the whole spectrum $P(\mathscr{E})$ and assuming for it a gaussian shape.

We have approximately, when $\psi = \left(\frac{d^2 \log T(\mathscr{E})}{d\mathscr{E}^2}\right)_{\mathscr{E}=\mathscr{E}^*}$:

$$P(\mathscr{E}) \alpha T(\mathscr{E}^*) \frac{e^{2\sqrt{aU^*}}}{U^{*5/4}} \cdot e^{\frac{\psi}{2}(\mathscr{E}-\mathscr{E}^*)^2 - \frac{\sqrt{a}}{4U^{*3/2}}(U-U^*)^2} \alpha e^{-(\mathscr{E}-\mathscr{E}^*)^2/2\sigma^2} . \tag{13}$$

TABLE VII

φ^* values

	U^{235}+neutrons$_{thermal}$	U^{235}+neutrons$_{6\ MeV}$	U^{235}+neutrons$_{15.5\ MeV}$
A_1	φ^* (MeV^{-1})	φ^* (MeV^{-1})	φ^* (MeV^{-1})
84	1.06	1.02	0.90
90	0.95	0.85	0.77
96	0.93	0.84	0.71
102	1.06	0.93	0.74
106	0.96	0.87	0.66
112	0.86	0.81	0.72
118	1.03	0.92	0.93

We obtain directly from the formula (13):

$$\psi = \frac{1}{2}\sqrt{\frac{a}{\overline{U}'^3}} - \frac{1}{\sigma^2} . \tag{14}$$

Taking into account the given values of a and the experimental values of $\overline{U}'$ and σ^2, from formula (14) we obtain the values of ψ which are given in Table VIII in correspondence with the various excitation energies of U^{236} and the various fragment pairs.

Even taking into account the incertitude on ψ values due to the various possible errors, it appears clearly that the ψ values are rather small with respect to φ^* and reduce pratically to zero at the higher excitation energies.

The expression for $T(\mathscr{E})$ is finally given by:

$$T(\mathscr{E}) = T(\mathscr{E}^*) e^{\varphi^*(\mathscr{E}-\mathscr{E}^*) + \frac{\psi}{2}(\mathscr{E}-\mathscr{E}^*)^2} . \tag{15}$$

This expression of $T(\mathscr{E})$ refers to the energy interval corresponding to an experimental spectrum region centered around $\mathscr{E}^*$.

For a more accurate analysis it should be observed that the experimental spectrum has a small asymmetry and has wings a bit higher than the gaussian curve; these details could be obtained by refining the calculation and developing the series to higher terms.

5.3. Shape of the two body potential

When the expression for $T(\mathscr{E})$ is obtained ,it is then possible, by means of formula (11), to deduce the shape of the two body potential $V(r)$ acting between the two fragments.

It will be useful to discuss briefly a few simple cases of potential barriers in order to deduce the shape of the potential barrier (Fig. 8) corresponding to the obtained transparency:

a) the coulombian barrier with infinite attractive potential.

The predicted barrier is given by:

$$V(r) = \frac{Z_1 Z_2}{r} e^2 \text{ for } r > R_0; V = -\infty \text{ for } r < R_0.$$

The transparency will be [28]:

$$T_c(\mathscr{E}) \alpha\, e^{-2x} \tag{16}$$

with

$$x = \frac{0.147\, R}{(A_1 + A_2)^{1/2}} (A_1 A_2)^{1/2} \frac{1}{\sqrt{\mathscr{E} B}} (B - \mathscr{E})^{3/2}.$$

B being the top of the barrier.

It results that, if the log $T_c(\mathscr{E})$ is developed up to the second order, the second derivate at $\mathscr{E} = \mathscr{E}^*$ has a sign opposite to the experimentally obtained values for ψ. This means that the transparency of the coulombian barrier varies too rapidly with the kinetic energy and consequently the energy spectra calculated with the coulombian transparency should result too narrow. This point was already cleared by Newton in 1956 [28].

b) The parabolic barrier, given by

$$V = B - \frac{1}{2} K(r - r_p)^2$$

r_p being the radius corresponding to the top B and K a suitable coefficient; its transparency is simply expressed by

$$T(\mathscr{E}) = e^{-\varphi(B - \mathscr{E})} \tag{17}$$

where: $\varphi = \frac{2\pi}{\hbar} \sqrt{\frac{M}{K}}$; in this case $\psi = 0$.

From comparison with Table VIII we see that, in the case of fission induced by 15.5 MeV neutrons, ψ is rather small, the barrier of the parabolic type is quite close to the one represented by these values of ψ.

c) The empirical barrier.

From Table VIII it appears that the ψ values are positive and have values of $\sim 10^{-2}$ MeV^{-2} for thermal neutron fission and of $\sim 5\ 10^{-3}$ MeV^{-2} for 6 MeV neutron induced fission respectively. These values of ψ correspond to the fact that the empirical barriers are steeper than the parabolic one and closer to a rectangular potential barrier.

We want to recall here that the expression (15) for $T(\mathscr{E})$ is referred to the values of $\mathscr{E}$ centered around the maximum of the experimental spectrum, so that we have no direct

TABLE VIII

ψ values

U^{235}+neutrons$_{thermal}$		U^{235}+neutrons$_{6\,MeV}$	U^{235}+neutrons$_{15.5\,MeV}$
A_1	ψ [MeV^{-2}]	ψ [MeV^{-2}]	ψ [MeV^{-2}]
84	$2.8\ 10^{-3}$	$1.1\ 10^{-3}$	$-7.6\ 10^{-3}$
90	$5.5\ 10^{-3}$	$1.0\ 10^{-3}$	$-1.2\ 10^{-3}$
96	$7.7\ 10^{-3}$	$3.0\ 10^{-3}$	$1.1\ 10^{-3}$
102	$17.0\ 10^{-3}$	$8.8\ 10^{-3}$	$0.0\ 10^{-3}$
106	$14.4\ 10^{-3}$	$9.0\ 10^{-3}$	$1.0\ 10^{-3}$
112	$8.1\ 10^{-3}$	$3.5\ 10^{-3}$	$0.0\ 10^{-3}$
118	$1.1\ 10^{-3}$	$5.0\ 10^{-3}$	$4.0\ 10^{-3}$

information on the barrier shape above this region and in the top region in particular. We cannot therefore obtain the detailed shape of the barrier in the top region.

In what follows, for sake of simplicity, we assume that ψ values remain constant *versus* $\mathscr{E}$ up to the top value B. Under this condition the whole expression for transparency $T(\mathscr{E})$

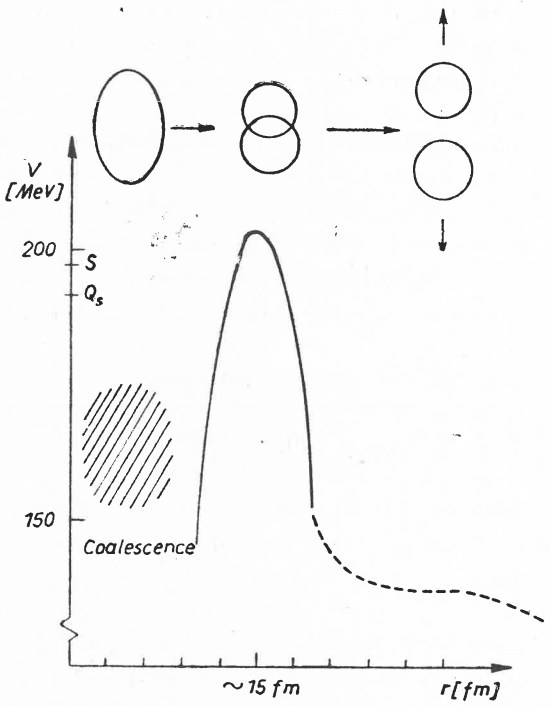

Fig. 8. Empirical potential barrier acting between the two fragments during the fusion process The potential is plotted *versus* r, distance between the centres of the two fragments. Schematic rapresentation of the intermediate configuration. The Q_s value, for fragment pair $A_1 = 96$, $A_2 = 140$ for spontaneous fission, and the value S of saddle point energy are indicated

becomes

$$T(\mathscr{E}) = e^{-\varphi_B(B-\mathscr{E}) + \frac{\psi}{2}(B-\mathscr{E})^2} \tag{18}$$

φ_B being the logarithmic derivative of $T(\mathscr{E})$ evaluated at the top B. φ_B is given by:

$$\varphi_B = \varphi^* + \psi(B - \mathscr{E}^*). \tag{18'}$$

Assuming the given values of φ^* and ψ it is possible to note that the width of these barriers at energies of 50 MeV under the top, is of the order of $2f$. It is also important to note that with increasing excitation of the compound nucleus the ψ value decreases, and correspondingly the shape of the barriers changes and approaches the parabolic shape.

5.4. Height of the barrier and mass spectra

Formula (8) allows us to relate the absolute values of the fission widths for a given fragment pair to the value of the B, the top of the fusion barrier. In fact, by assuming the parabolic barrier we obtain the simplified formulae:

$$P_m \frac{\Gamma_I}{D_I} \approx P_m \frac{\Gamma_0}{D_0} = \sqrt{\frac{2}{\pi}} \frac{1}{12^2} \frac{1}{\sqrt{X}} \frac{a}{a_1 a_2} \frac{1}{\bar{U}'} e^{2\sqrt{a\bar{U}'} - \varphi_B(B-\mathscr{E}^*) + \frac{\psi}{2}(B-\mathscr{E}^*)^2} \tag{19}$$

$$X = 0.146 \sqrt{\frac{\bar{U}'}{a}} \sum_i a_i A_i^{5/3}; \text{ being } 2\sqrt{a\bar{U}'} = 2\bar{U}'\varphi^* + \frac{7}{2}.$$

Formula (19) indicates that the fission widths for the different fragment pairs and the shape of the mass spectra are very sensitive to B values. 1 per cent variation of B produces an effect 3 times greater in the fission probability of a given fragment pair.

In some way it is therefore impossible to attempt a prediction of the mass spectra on the basis of the knowledge of the values of B, as the B values are not known with great accuracy.

TABLE IX

Values of the parabolic barrier height B

U^{235}+neutrons thermal			U^{235}+neutrons 6 MeV	U^{235}+neutrons 15.5 MeV	
A_1	Z_1	B [MeV]	B [MeV]	B [MeV]	Vc_{16f} [MeV]
84	34	206.0	206.0	212.0	189.3
90	36	205.0	203.0	199.0	193.5
96	38	210.0	206.5	203.0	197.0
102	40	210.0	209.5	215.0	199.7
106	42	215.5	211.0	212.0	201.6
112	44	223.0	220.5	221.5	202.7
118	46	208.5	209.0	206.5	203.1

The errors in the B values are estimated to be ± 10 MeV, due to the uncertainties in the experimental data.

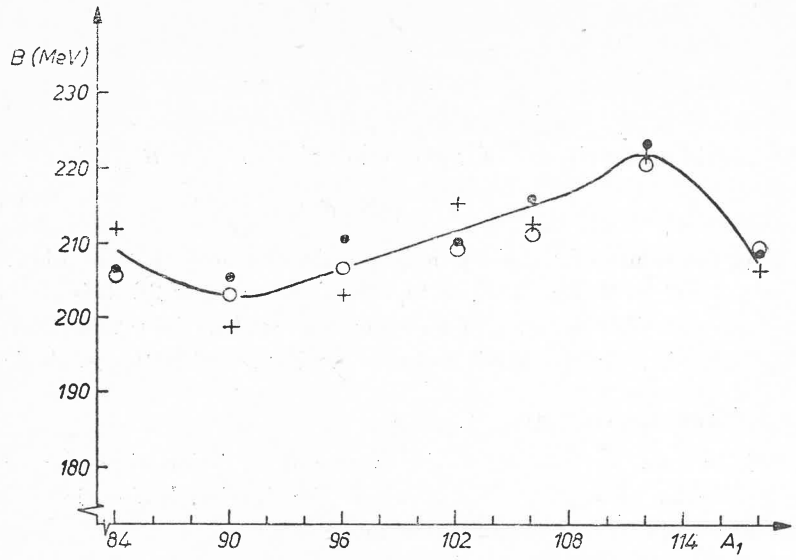

Fig. 9. Obtained B values for fission of U^{235} induced by thermal neutrons: black points, by 6 MeV neutrons: light points, by 15.5 MeV neutrons: crosses.

On the other hand, it is possible to check which values of B can reproduce the experimental mass spectra. By introducing a, $\overline{U}$ and φ^* and ψ values of the tables we obtain from formula (19) the B values shown in Table IX and in Fig. 9. B values prove to be of the order of 210 MeV and they vary slowly for the various fragment pairs. In Table IX also the values of the coulomb potential calculated at $r = 16\ f$ are given.

It is interesting to note that B is practically constant when the excitation energy of the compound nucleus increases.

6. Fusion and scission dynamical barriers

The analysis carried out in the preceding paragraphs has shown that the fusion of two excited fragments undergoes a tunnelling effect through a sharp potential barrier of an almost parabolic shape.

The top of the barrier is around 210 MeV and the barrier extends, with quasi parabolic shape, down to 150 MeV, *i. e.* to the lower limit of the kinetic energy spectrum of the fragments.

We have now to establish at which distances this barrier acts and in which way it is connected at large distances with the coulombian potential. This coulombian potential starts from zero at infinite distance and increases as r^{-1} as the fragments approach each other; it reaches values around 150 MeV at distances of the order of 20–22 fermi. According to what has been assumed, deviation from the coulombian law should begin at this distance.

It does not seem possible, however, that the sharp repulsive barrier acts at 22 fermi, when the two fragments are not yet in a strong contact.

The model for the potential presented is the following: the long range tails of the

attractive nuclear forces begin nuclear interactions in the region at 20–22 fermi; interactions can take place at these distances by means either of vibrations or of deformations of the fragments and as the fragments approach each other the increased nuclear attractive forces balance the increase of the repulsive coulombian potential; a rather flat potential region is formed.

At smaller distance, when the fragments cores come into closer contact, strong repulsive forces intervene and the whole potential starts to rise steeply and assumes the predicted quasi parabolic shape. The top B of the barrier can be tentatively located at distances of the order of 15 fermi.

A potential having these features has been pointed out in the $C^{12}+C^{12}$ collision process by Vogt and Mc Manus [29] *etc.* and recently in the $O^{16}+O^{16}$ collision processes by Block and Malik [30].

The whole expression of the potential (Fig. 8) is given by

$$V = V_C + V_N + V_R$$

where V_N is the attractive part, V_R the repulsive part of the nuclear forces and V_C the coulombian potential. In order to have the flat potential region, the V_N value must be at least of the order of 30 MeV (Fig. 8). If the top B is supposed to be located at about 15 fermi, we have $V_C \simeq 200$ MeV and correspondingly V_R should prove of the order of 50–70 MeV.

Let us now consider the nature of the repulsive forces. In a recent work, various authors, *i. e.* Greiner *et al.* [31] and Sona and Erba [32[assume that in the coalescence process of two heavy nuclei there can be regions where the two nuclei are partially superimposed with nuclear densities greater than their usual values.

This effect produces, repulsive forces, which according to calculations of Sona and Erba [32], are of the order of 50 MeV/fermi. The two fragments under collision pass through these configurations of anomalous density and are affected by the strong repulsive forces (Fig. 8).

The descent of the barrier in the compound nucleus region can be due to the forces originated by rearrangement of the nuclear shells; in fact in the coalescence process the nucleons present in the two fragments, change their orbit and reduce their total energy.

As the process is reversible it can be also considered, from the viewpoint of the compound nucleus, *i. e.* in the scission process. The corresponding scheme for scission is the following: the rearrangement of the shells represents the barrier rise that the compound nucleus meets for the scission. It is interesting to note that the barrier is $\approx$ 10 MeV above the region of Bohr saddle.

The two fragments configurate in their internal structure, and with the given excitation energy, and suddenly blow up passing under the barrier for tunnelling effect. Their kinetic and excitation energies are determined by the channel number and by the penetrability factor.

This scheme is given in first approximation: a thorough analysis both for scission and fusion should take into account possible deformations of the fragments in the final states and the corresponding deformation energies.

The part of the barrier near the top where the Pauli forces act could depend on the state

configurations of the compound nucleus and consequently on its excitation. At the highest excitations the rearrangement of the nuclear shells gradually reduces owing to the large number of states, which are available in the compound nucleus. This effect may explain the fact that the shape of the barrier changes slightly when the compound nucleus excitation energy increases.

As the described barrier represents the configurations which the system assumes in the sudden dynamic process of scission and fusion, we indicate it as dynamical scission and fusion barrier in order to distinguish it from the Bohr saddles describing uniform deformations of the nuclei.

We can therefore conclude our analysis by observing that, though transparency $T(\mathscr{E})$ is very small, the product of transparency by the large number of the final channel $I(U)$ gives values of Γ_f well fitted to experimental values: the sudden process can therefore be dominant. The proposed model should apply even when the initial system is below the saddle, as, for instance, in the spontaneous fission of U^{236}. In fact the energy spectra of the fragments in the spontaneous fission show the same shape and width as discussed for the fission induced by neutron capture. The system, owing to the tunnelling effect, goes both under the deformation saddle and under the scission dynamical barrier.

A more refined model should take into account the fact that the fragments are not two single bodies, but sets of nucleons, transparency then should be calculated with more complicated and general formulae.

It is however interesting to note that the simple model of a two body potential barrier, allows a good description of the basic properties of the fission fragments of heavy nuclei.

REFERENCES

[1] L. Wilets, *Theory of nuclear fission*, Clarendon Press, Oxford 1964.
[2] W. I. Swiatecki, SM60/1 *Proceeding of physics and chemistry fission*, Salzburg 1965.
[3] N. Bohr, I. A. Wheeler, *Phys. Rev.*, **56**, 426 (1939).
[4] S. Cohen, W. J. Swiatecki, *Ann. Phys.*, **22**, 406 (1963).
[5] V. M. Strutinsky, *Nuclear Phys.*, **A95**, 420 (1967).
[6] G. N. Flerov, S. M. Polikanov, *Comptes Rendus du Congress International de Physique Nucleaire*, Paris **1**, 407 (1964).
[7] G. N. Flerov, S. M. Polikanov, S. P. Tretyakova, N. Martalogu, D. Paenaru, M. Sezon, I. Vilcov, N. Vilcov, *Nuclear Phys.*, **A97**, 444 (1967).
[8] E. Migneco, J. P. Theobald, *Nuclear Phys.*, **A112**, 603 (1968).
[9] D. Paya, J. Bloss, H. Derrien, A. Fubini, A. Michaudon, P. Ribon, *J. Phys.* (France), (1968).
[10] P. Fong, *Phys. Rev.*, **89**, 332 (1953).
[11] A. V. Ignatiuk, *Yadernaya Fizika* (URSS), **9**, 357 (1969).
[12] T. Ericson, *Advances in Phys.*, **9**, 36 (1960).
[13] E. Erba, U. Facchini *et. al.*, *Phys. Letters*, **6**, 294 (1963); E. Erba, U. Facchini, E. Saetta-Menichella, *Nuclear Phys.*, **84**, 595 (1966).
[14] U. Facchini, E. Gadioli Erba, E. Saetta-Menichella, *Phys. Letters*, **28B**, 534 (1969).
[15] H. W. Schmitt, J. H. Neiler, F. J. Walter, *Phys. Rev.*, **141**, 1146 (1966).
[16] G. Signarbieux, M. Ribrag, H. Nifenecker, *Nuclear Phys.*, **A99**, 41 (1967).
[17] V. G. Vorobeva, P. P. Dyachenko, B. D. Kuzminov, M. Z. Tarasko, *Yadernaya Fizika*, **4**, 325 (1966).
[18] P. Dyachenko, B. D. Kuzminov, *Yadernaya Fizika*, **7**, 36 (1968).

[19] J. Wing, J. Varley, *ANL 6886*, (1964).
[20] E. E. Maslin, A. L. Rodgers, W. G. F. Core, *Phys. Rev.*, **164**, 1520 (1967).
[21] V. F. Apalin *et. al.*, *Nuclear Phys.*, **55**, 249 (1964).
[22] M. Ribrag, *Theses*, *Rapport CEA*, R3309 1967.
[23] J. C. D. Milton, J. S. Fraser, *Proceedings of the physics and chemistry of fission symposium*, Salzburg, vol. II, 39, 1965.
[24] K. Parker, *AWRE 0 82/63*, 1963.
[25] E. Erba, U. Facchini, E. Saetta-Menichella, *Nuovo Cimento*, **22**, 1237 (1961).
[26] U. Facchini, E. Saetta-Menichella, *Energia Nucleare*, **15**, 30 (1968).
[27] D. W. Lang, *Nuclear Phys.*, **53**, 113 (1964).
[28] T. D. Newton, *Proc. Symposium on the Physics of fission Chalk River*, Report CRP-642-A; *Atomic Energy of Canada*, Report AECL 329 (1956).
[29] E. Vogt, H. McManus, *Phys. Rev. Letters*, **4**, 518 (1960).
[30] B. Block, E. B. Malik, *Phys. Rev. Letters*, **19**, 239 (1967).
[31] W. Scheid, R. Ligensa, W. Greiner, *Phys. Rev. Letters* **21**, 1479 (1968).
[32] E. Gadioli Erba, P. G. Sona, *Phys. Rev. Letters*, **22**, 406 (1969).